British Journal of Pharmacology (2006) 148, 162–172
www.nature.com/bjp

Residues in the first transmembrane domain of the *Caenorhabditis elegans* $GABA_A$ receptor confer sensitivity to the neurosteroid pregnenolone sulfate

[1]Bryan Wardell, [1]Purba S. Marik, [2]David Piper, [3,4]Tina Rutar, [3]Erik M. Jorgensen & *,[1]Bruce A. Bamber

[1]Department of Pharmacology and Toxicology, University of Utah, 30 South 2000 East, Salt Lake City, UT 84112, U.S.A.; [2]Department of Physiology, University of Utah, 410 Chipeta Way, Salt Lake City, UT 84108, U.S.A. and [3]Department of Biology, University of Utah, 257 South, 1400E Salt Lake City, UT 84112, U.S.A.

1 The $GABA_A$ receptor is a target of endogenous and synthetic neurosteroids. Little is known about the residues required for neurosteroid action on $GABA_A$ receptors. We have investigated pregnenolone sulfate (PS) inhibition of the *Caenorhabditis elegans* UNC-49 GABA receptor, a close homolog of the mammalian $GABA_A$ receptor.

2 The UNC-49 locus encodes two GABA receptor subunits, UNC-49B and UNC-49C. UNC-49C is sensitive to PS but UNC-49B is not sensitive. By analyzing chimeric receptors and receptors containing site-directed mutations, we identified two regions required for PS inhibition.

3 Four residues in the first transmembrane domain are required for the majority of the sensitivity to PS, but a charged extracellular residue at the end of the M2 helix also plays a role. Strikingly, mutation of one additional M1 residue reverses the effect of PS from an inhibitor to an enhancer of receptor function.

4 Mutating the M1 domain had little effect on sensitivity to the inhibitor picrotoxin, suggesting that these residues may mediate neurosteroid action specifically, and not allosteric regulation in general.
British Journal of Pharmacology (2006) **148,** 162–172. doi:10.1038/sj.bjp.0706719;
published online 20 March 2006

Keywords: $GABA_A$ receptor; neurosteroid; pregnenolone sulfate; modulatory site; *unc-49*; *Caenorhabditis elegans*

Abbreviations: ANOVA, analysis of variance; DMSO, dimethyl sulfoxide; GABA, γ-aminobutyric acid; IQR, interquartile range; PCR, polymerase chain reaction; pregnanolone, 5β-pregnan-3α-ol-20-one; PS, pregnenolone sulfate; s.e.m., standard error of the mean

Introduction

Neurosteroids are endogenous steroid molecules, synthesized in the brain, which play important physiological roles. Neurosteroids influence such nervous system functions as seizure susceptibility, anxiety, responses to stress and ethanol, and learning and memory (Vallee *et al*., 1997; Mellon & Griffin, 2002; Rupprecht, 2003; Morrow *et al*., 2004). Physiological effects of neurosteroids are mediated mainly by $GABA_A$ receptors (Belelli & Lambert, 2005), which are the principal inhibitory neurotransmitter receptors in the brain (Macdonald & Olsen, 1994). $GABA_A$ receptor function is enhanced by some neurosteroids, such as pregnanolone, but inhibited by others, such as pregnenolone sulfate (PS; Paul & Purdy, 1992). Other neurotransmitter receptors are also sensitive to neurosteroid modulation. For example PS enhances *N*-methyl-D-aspartate receptor function (Wu *et al*., 1991). Synthetic neurosteroids have shown promise as drugs to treat neurological disorders such as insomnia, migraine, anxiety, and epilepsy (Gasior *et al*., 1999; Kerrigan *et al*., 2000; Laxer *et al*., 2000).

The mechanisms by which neurosteroids modulate $GABA_A$ receptor function are not well understood. Residues important for the actions of other allosteric regulators of $GABA_A$ receptors affect neurosteroid modulation as well (Akk *et al*., 2001; Chang *et al*., 2003; Morris & Amin, 2004). Thus, neurosteroids appear to use some of the same general mechanisms to modulate $GABA_A$ receptor function as other allosteric regulators. However, it is likely that other $GABA_A$ receptor residues mediate neurosteroid action specifically, for example, by forming a neurosteroid binding pocket. Further, there is evidence to suggest that the mechanisms of neurosteroid enhancement and inhibition are different (Zaman *et al*., 1992; Park-Chung *et al*., 1999), suggesting that some receptor residues may play roles specific to individual neurosteroids. These neurosteroid-specific residues have not yet been identified. In this study, we identify residues of $GABA_A$ receptor important for neurosteroid modulation, but not necessarily for the actions of other drugs.

These studies rely on differential drug sensitivities of $GABA_A$ receptor subunits in the nematode *Caenorhabditis elegans*. The gene *unc-49* encodes multiple GABA receptor subunits (Bamber *et al*., 1999) that are closely related to mammalian $GABA_A$ receptors (Bamber *et al*., 2003). Like

*Author for correspondence; E-mail: bamber@hsc.utah.edu
[4]Current address: Department of Ophthalmology, University of California, San Francisco, CA 94143, U.S.A.

their mammalian homologs, UNC-49 subunits contain a large extracellular amino terminal region, and four transmembrane domains labeled M1–M4. Five subunits assemble to form a pentameric chloride channel, with the M2 domain from each subunit contributing the pore-lining residues (reviewed in Olsen & Tobin, 1990). *In vivo*, UNC-49B coassembles with UNC-49C to form a GABA$_A$ receptor that functions at the neuromuscular junction to permit coordinated locomotion (Bamber *et al*., 2005). However, UNC-49B subunits (but not UNC-49C subunits) can also efficiently form homomeric receptors. The *C. elegans* GABA receptor is neurosteroid sensitive. Both UNC-49B homomers and UNC-49B/C heteromers are, atypically, inhibited by pregnanolone (Bamber *et al*., 2003). Interestingly, the two forms of this receptor show differential PS sensitivity: PS inhibits the UNC-49B/C heteromer much more strongly than the UNC-49B homomer. This finding suggests that UNC-49C contains sequences important for PS modulation. By swapping residues from UNC-49C into UNC-49B we converted this PS-insensitive receptor into a PS-sensitive receptor. First, we created chimeras of these two subunits to demonstrate that the M1 and M2–M3 linker domains are important for PS sensitivity. Second, we demonstrated roles for residues within these domains that are conserved among neurosteroid-sensitive receptors but divergent in UNC-49B. Third, using systematic mutagenesis of the M1 domain, we identified additional residues that control PS sensitivity. Mutations in critical M1 residues have little or no effect on the sensitivity of the receptor to the allosteric inhibitor picrotoxin, suggesting that we have identified residues with a specific role in GABA receptor modulation by neurosteroids.

Methods

Sequence analysis and modeling

To identify conserved residues for mutagenesis, the following cysteine loop receptor subunits were aligned: Rat GABA$_A$ receptor subunits α1 (SwissProt: p18504), α2 (SwissProt: p23576), α3 (SwissProt: p20236), α4 (SwissProt: p28471), α5 (SwissProt: p19969), α6 (SwissProt: p30191), β1 (SwissProt: p15431), β2 (SwissProt: p15432), β3 (SwissProt: p15433), γ1 (SwissProt: p23574), γ2 (SwissProt: p18508), γ3 (SwissProt: p28473), δ (SwissProt: p18506); Rat GABA$_C$ receptor subunits ρ1 (SwissProt: p50572), ρ2 (SwissProt: p47742), ρ3 (SwissProt: p50573); Rat glycine receptor subunits α1 (SwissProt: p07727), α2 (SwissProt: p22771), α3 (SwissProt: p24524), β (SwissProt: p20781); Human GABA$_A$ receptor ε subunit (gb:U66661), *Drosophila melanogaster rdl* gene product (SwissProt: p25123), *Drosophila* GABA receptor β subunit (SwissProt: q08832); *lymnaea stagnalis* GABA receptor β subunit (SwissProt: p26714); and avermectin-sensitive glutamate-gated chloride channel α1 subunit (pir2:s50864), β subunit (gb:u14525). Alignment was performed using the Pileup program in the GCG computer sequence analysis package.

Homology models were built using ModellerV6.2 (Sali & Blundell, 1993) based on the 4 Å structure of the nicotinic acetylcholine receptor transmembrane domains (Miyazawa *et al*., 2003). The following subunits were aligned to generate this model: *Torpedo marmorata* nicotinic acetylcholine receptor subunits α (1OEDA), β (1OEDB), δ (1OEDC), γ (1OEDE); mouse nicotinic acetylcholine receptor α1 subunit (P04756); UNC-49B (AAD42383), rat GABA$_A$ receptor subunits α1 (P18504), α2 (P23576), α3 (P20236), α4 (P28471), β1 (P15431), β2 (P15432), β3 (P15433), γ1 (P23574), γ2 (P18508), γ3 (P28473), rat GABA$_C$ receptor subunits ρ1 (P50572), ρ2 (P47742), ρ3 (P50573); rat glycine receptor subunits α1 (P07727), α2 (P22771), α3 (P24524), β (P20781); human GABA$_A$ receptors α5 (CAA01920), α6 (NP000802), *D. melanogaster Rdl* gene product (P25123). Membrane-spanning residues were aligned, the large intracellular loop between M3 and M4 was omitted. Alignments were performed with ClustalW software (Thompson *et al*., 1994).

Site-directed mutagenesis

Chimeric and mutant receptors were constructed using standard molecular biology techniques. Construction of chimeras and site-directed mutagenesis were performed using a polymerase chain reaction (PCR)-based method. Briefly, mutations were introduced into the sequences of oligonucleotide primers used for PCR. The resulting PCR products were then cloned into either a wild-type or mutagenized UNC-49B plasmid to generate the desired combination of mutations and chimeric segments. Silent restriction sites were often introduced at convenient locations, also using the PCR-based mutagenesis procedure, to facilitate plasmid construction. For each new molecule, the region corresponding to the mutagenized PCR fragment, and its junctions with the vector molecule, were sequenced prior to use.

Electrophysiology

Plasmids containing wild-type and mutagenized GABA$_A$ receptor subunits were linearized and transcribed *in vitro* using T3 RNA polymerase (mMessage mMachine T3 kit, Ambion, Austin, TX, U.S.A.). UNC-49B mRNA was injected into *Xenopus laevis* oocytes at $0.5\,\mu g\,\mu l^{-1}$ either alone, or in a mixture with $0.5\,\mu g\,\mu l^{-1}$ UNC-49C. All other *C. elegans* subunits were injected at $1.0\,\mu g\,\mu l^{-1}$ except for the TM chimera, which produced very small currents and was injected at concentrations up to $6.0\,\mu g\,\mu l^{-1}$. The injection volume ranged between 27.6 and 50.6 nl. Oocytes were analyzed using two electrode voltage-clamp electrophysiology using a GeneClamp 500 Amplifier (Axon Instruments, Foster City, CA, U.S.A.), as previously described (Bamber *et al*., 2003). Cells were voltage clamped at -60 mV. All recordings were performed at room temperature.

GABA EC$_{50}$ concentrations were determined by performing GABA dose–response curves, and fitting them with the equation:

$$I = I_{max}/\{1 + 10^{(\log EC_{50} - [agonist]) \times n}\}$$

where I is current at a given GABA concentration, I_{max} is current at saturation, EC$_{50}$ is the GABA concentration required to produce half-maximal current, and n is the slope coefficient. GABA dose–response curves were fit using GraphPad Prism software (San Diego). PS inhibition was measured at the GABA EC$_{50}$ concentration for all receptors, with the exception of the M1–M2 chimera and the M1–M2-linker chimera. These molecules expressed very inefficiently, producing no current in most cells, and only small currents in others. First, it was difficult to obtain enough expressing cells to accurately determine GABA EC$_{50}$ values. Second, it was necessary to use high GABA concentrations to obtain currents

Table 1 GABA and PS responsiveness of wild-type and chimeric UNC-49 receptors

Subunit	*PS*		*GABA*	
	IC_{50} (μM)	*Slope coefficient*	EC_{50} (μM)	*Slope coefficient*
UNC-49B	191	0.7	371±61 ($n=4$)	2.0±0.1 ($n=4$)
UNC-49B/C	2.3±0.2 ($n=4$)	0.9±0.1 ($n=4$)	750±31 ($n=4$)	1.3±0.1 ($n=4$)
TM chimera	ND	ND	119.7±17.8 ($n=5$)	1.1±0.1 ($n=5$)
M1–M2-linker chimera	ND	ND	20.3 ($n=2$)	0.7 ($n=2$)
M1–M2 chimera	ND	ND	>300 ($n=2$)	ND
M1 chimera	11.9±2.0 ($n=4$)[a,b]	0.9±0.1 ($n=4$)	290±48 ($n=5$)	1.7±0.1 ($n=5$)
Linker chimera	44.9±7.0 ($n=5$)[a,b]	1.3±0.2 ($n=5$)	9.7±1.5 ($n=5$)	2.0±0.2 ($n=5$)
double chimera (M1+linker)	3.6±0.3 ($n=4$)[c]	1.4±0.1 ($n=4$)	0.36±0.1 ($n=5$)	1.0±0.1 ($n=5$)
M1-R	2.8±0.4 ($n=8$)[d]	1.2±0.1 ($n=8$)	24.2±2.0 ($n=11$)	1.9±0.2 ($n=11$)
N305R	51.0±4.5 ($n=4$)[e]	1.9±0.2 ($n=4$)	4.0±0.5 ($n=7$)	2.0±0.2 ($n=7$)
QF-R	24.7±4.7 ($n=6$)[b,f]	1.5±0.5 ($n=6$)	8.0±1.8 ($n=10$)	1.8±0.1 ($n=10$)

ND not determined; Error values are s.e.m. PS IC_{50} values were determined at EC_{50} GABA.
[a]Significantly different from UNC-49B/C ($P<0.05$, Mann–Whitney U-test).
[b]Significantly different from double chimera ($P<0.05$, Mann–Whitney U-test).
[c]Significantly different from UNC-49B/C ($P<0.05$, Student's t-test).
[d]Not different from double chimera ($P>0.05$, Student's t-test).
[e]Not different from linker chimera ($P>0.05$, Student's t-test).
[f]Significantly different from N305R mutant ($P<0.05$, Student's t-test).

large enough to measure PS inhibition (1000 μM for the M1–M2 chimera and 100 μM for the M1–M2-linker chimera). For UNC-49B homomers and UNC-49B/C heteromers, GABA EC_{50} values are highly variable (Bamber *et al*., 2003). EC_{50} values presented in Table 1 for these two receptors reflect a single batch of oocytes that was used to measure the PS IC_{50}.

PS inhibition was measured by applying PS for 20 s, and then coapplying PS and GABA. PS preapplications (10 and 20 s) produced the same amount of inhibition, suggesting that the amount of PS bound to the receptor was no longer changing at the time that GABA was applied. Generally, PS evoked little or no direct response. For most constructs, PS preapplication resulted in changes in the holding current corresponding to <5% of EC_{50} GABA-evoked currents (upward or downward deflection, depending on the molecule), and only at the highest PS concentrations (30 and 100 μM). The T257F and T257F/S264A point mutants and the XY chimera were exceptions: application of 100 μM PS caused a reduction of the holding current (opposite to the effect of GABA) that was 6–20% as large as the EC_{50} GABA-evoked current for the T257F and T257F/S264A point mutants, and equal in amplitude to the EC_{50} GABA-evoked current for the XY chimera. Interestingly, picrotoxin did not depress these holding currents, suggesting that PS and picrotoxin may modulate different classes of open states. Where PS direct effects were observed, GABA-evoked peak currents were measured from the baseline in the presence of PS rather than the baseline prior to PS application. This correction resulted in PS IC_{50} values that were 44% higher for T257F, and 18% higher for T257F/S264A, but not significantly different for the XY chimera. Picrotoxin inhibition of GABA-evoked currents was measured by coapplication of GABA and picrotoxin. We routinely verified that currents recovered to their original magnitudes once the inhibitors had been removed. Currents reported in this study are the peak currents observed upon GABA application. PS and picrotoxin dose-response curves were fitted using the equation:

$$I_{inh+}/I_{inh-} = 1/\{([inh]/IC_{50})^n + 1\}$$

where I_{inh+}/I_{inh-} is the current in the presence of inhibitor (PS or picrotoxin) relative to GABA alone, IC_{50} is the concentration of inhibitor required to block 50% of the current, and n is the slope coefficient. PS dose–response curves were fit using GraphPad Prism or NFIT (Island Products, Galveston, TX, U.S.A.; Figure 1c UNC-49B/C curve only). Biphasic dose–response curves (Figure 5) were fit with the equation:

$$I = [1 + A/(1 + (EC_{50}/[PS])^{nE})] \times [1/(([PS]/IC_{50})^{nI} + 1)]$$

where I is normalized current, A is the amplitude of I above 1, EC_{50} and IC_{50} are, respectively, the half-maximal enhancing and inhibitory concentrations of PS, nE and nI are, respectively, the slope coefficients for the enhancement and inhibition. Biphasic PS dose–response curves were fit with MATLAB (The MathWorks, Natick, MA, U.S.A.), using custom-written routines (M. Jones, University of Wisconsin, Madison, WI, U.S.A.). Confidence limits were estimated using a bootstrapping approach with 1000 trials (Jones *et al*., 2001). These trials generated the following median parameter values and interquartile ranges (IQR): For the M258L mutant, $A=1.56$ (IQR = 1.0–5.4), $EC_{50}=3.95\,\mu$M (IQR = 2.0–16.8), nE = 1.0 (IQR = 0.7–1.1), $IC_{50}=45.3\,\mu$M (IQR = 25.0–57.0), and nI = 1.8 (IQR = 1.5–2.1). For the M258L/S264A mutant, $A=1.0$ (IQR = 0.6–3.2), $EC_{50}=2.4\,\mu$M (IQR = 1.3–8.6), nE = 1.3 (IQR = 0.9–1.9), $IC_{50}=52.6\,\mu$M (IQR = 25.0–71.0), and nI = 1.9 (IQR = 1.4–2.6). Error bars in the figures are standard error of the mean (s.e.m.). All drugs were obtained from Sigma (St Louis, U.S.A.). GABA was prepared as a 1 M stock in water, and stored at −20°C for up to 1 year. PS was prepared as 10 mM stocks in dimethyl sulfoxide (DMSO). The final DMSO concentration was 1% at the maximal PS concentrations tested, and we verified that this concentration of DMSO did not inhibit or enhance GABA-evoked currents. Picrotoxin was prepared as a 100 mM stock in DMSO.

Results

The UNC-49C subunit confers increased PS sensitivity

The UNC-49B/C heteromer is significantly more sensitive to PS inhibition than the UNC-49B homomer (Figure 1, Table 1).

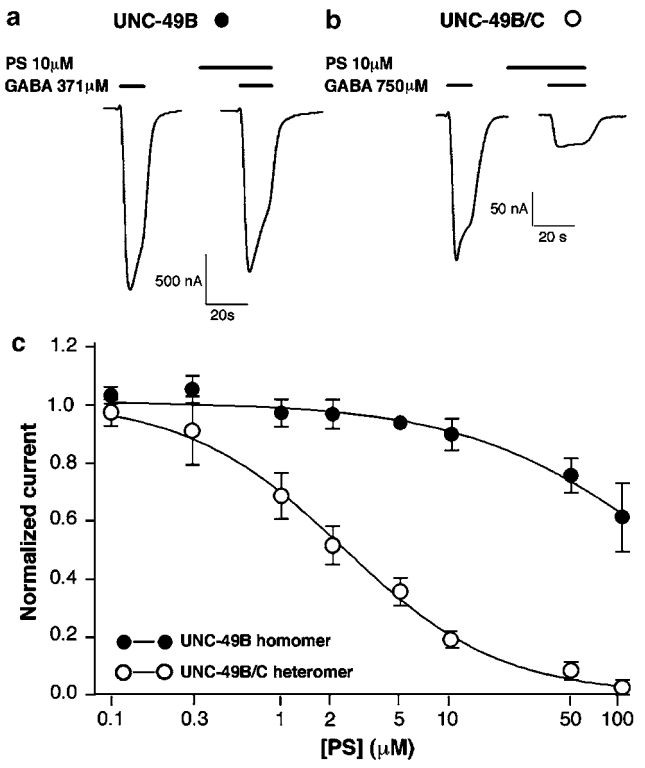

Figure 1 The UNC-49B/C heteromer is more sensitive to PS inhibition than the UNC-49B homomer. PS (10 μM) inhibition of GABA-evoked currents from *Xenopus* oocytes expressing UNC-49B homomeric GABA receptors (a) or UNC-49B/C heteromeric receptors (b). PS was preapplied for 20 s prior to coapplication of PS and GABA (at EC_{50}). (c) PS dose–response curves for UNC-49B homomers and UNC-49B/C heteromers. Peak currents evoked by EC_{50} GABA plus PS, normalized to currents evoked by GABA alone, are plotted against PS concentration. Error bars represent s.e.m. ($n=4$ oocytes for each receptor).

UNC-49B/C heteromeric receptors were inhibited by 95% at 100 μM PS, and the PS concentration that produced half-maximal inhibition (IC_{50}) was 2.3 μM. This value is very similar to inhibition observed for mammalian GABA$_A$ receptors which is also in the low micromolar range (Majewska, 1992; Nilsson *et al*., 1998; Park-Chung *et al*., 1999; Shen *et al*., 1999). By contrast, the UNC-49B homomer displayed only modest inhibition (40%) at 100 μM PS. By extrapolating the PS dose–response curve, we estimate the PS IC_{50} for UNC-49B homomers to be 191 μM.

One interpretation of this differential PS sensitivity is that UNC-49C contributes residues which bind PS with higher affinity, or transduce PS binding into channel inhibition more efficiently than their UNC-49B counterparts. We designed a three-step approach to identify these UNC-49C residues: first, we constructed chimeric subunits to identify the regions of UNC-49C which contain the critical residues; second, we identified residues in these regions which were conserved with other neurosteroid-sensitive subunits that played a role in PS sensitivity; and third, we performed systematic mutagenesis to identify the remaining contributors to PS sensitivity.

Domains required for PS inhibition

The increased PS sensitivity of the UNC-49C-containing receptor suggested that domains important for PS inhibition might be identified using a chimera approach. We constructed a series of chimeric subunits containing UNC-49B and UNC-49C sequences. UNC-49B and UNC-49C are generated by alternative splicing of a single gene (*unc-49*) that contains a shared amino terminus and three alternative carboxy termini (Bamber *et al*., 1999). The common amino terminus is 188 amino acids long, and includes some of the residues which form the GABA binding site (binding segments A, D, and E; Lester *et al*., 2004). The divergent regions encompass the remaining residues of the GABA binding site (binding segments B, C, and F; Lester *et al*., 2004), and all four transmembrane domains (Figure 2a). The following chimera experiments demonstrate that important determinants of PS inhibition are located in the M1 domain and in the linker joining M2 and M3.

We first tested the entire transmembrane domain region of UNC-49C. We constructed a chimera that contained the entire extracellular domain derived from UNC-49B, and transmembrane domain sequences derived from UNC-49C (the 'TM' chimera). The TM chimera formed a functional homomer that was strongly inhibited by 5 μM PS (Figure 2b, Table 1). This result is significant for two reasons. First, it demonstrates that important residues for PS inhibition are located within the transmembrane domain region of UNC-49C. Second, it demonstrates that the UNC-49C PS site can function in a homomultimeric configuration. This property simplifies further analysis: mutational analysis in heteromultimers is complicated by the possibility that mutations can alter subunit stoichiometry, rather than simply PS interactions. From this point forward, all chimeric and mutant subunits were analyzed as homomultimers.

To narrow the UNC-49C residues that are necessary for increased PS sensitivity, we tested progressively smaller stretches of the UNC-49C transmembrane domain region. The strategy represents a deletion of UNC-49C material from the carboxy to amino terminal end of the transmembrane portion of the subunit, which is then replaced with UNC-49B sequences. First we tested the M1 through the M2–M3 linker of UNC-49C for PS sensitivity (Figure 2b, 'M1–M2-linker' chimera). This chimera was equally sensitive to 5 μM PS as the TM chimera, indicating that UNC-49C residues from the beginning of M3 to the C terminus were dispensible for high PS sensitivity. By contrast, a chimera including only the first two transmembrane regions of UNC-49C ('M1–M2' chimera) was significantly less PS sensitive, indicating that the UNC-49C M2–M3 linker was necessary for high PS sensitivity. A chimera composed of the first transmembrane domain (the 'M1' chimera) did not have further reduced PS sensitivity, showing that UNC-49C M2 domain was not necessary for PS sensitivity. However, the M1 chimera was significantly more PS sensitive than the wild-type UNC-49B receptor, indicating a role for the UNC-49C M1 residues. These data suggest that two regions are required for PS sensitivity: the M2–M3 linker domain and the M1 transmembrane domain.

We then demonstrated that the M1 and M2–M3 linker domains together are sufficient for full PS sensitivity. We compared a construct containing both domains to constructs containing just one of these domains (Figure 2b and c). PS sensitivity was assessed in this and all subsequent experiments by generating PS dose-response curves and comparing IC_{50} values. The UNC-49C M2–M3 linker alone (the 'linker'

chimera) modestly increased PS sensitivity. The UNC-49C M1 domain alone increased PS sensitivity to a greater degree, but was still insufficient to increase PS sensitivity to the same level as the UNC-49B/C heteromer. However, when substituted together (the 'double' chimera), these two domains conferred PS sensitivity that was only slightly less than the UNC-49B/C heteromer. Therefore, residues in the M1 domain and the M2–M3 extracellular linker are sufficient to account for nearly all of the PS sensitivity of UNC-49C.

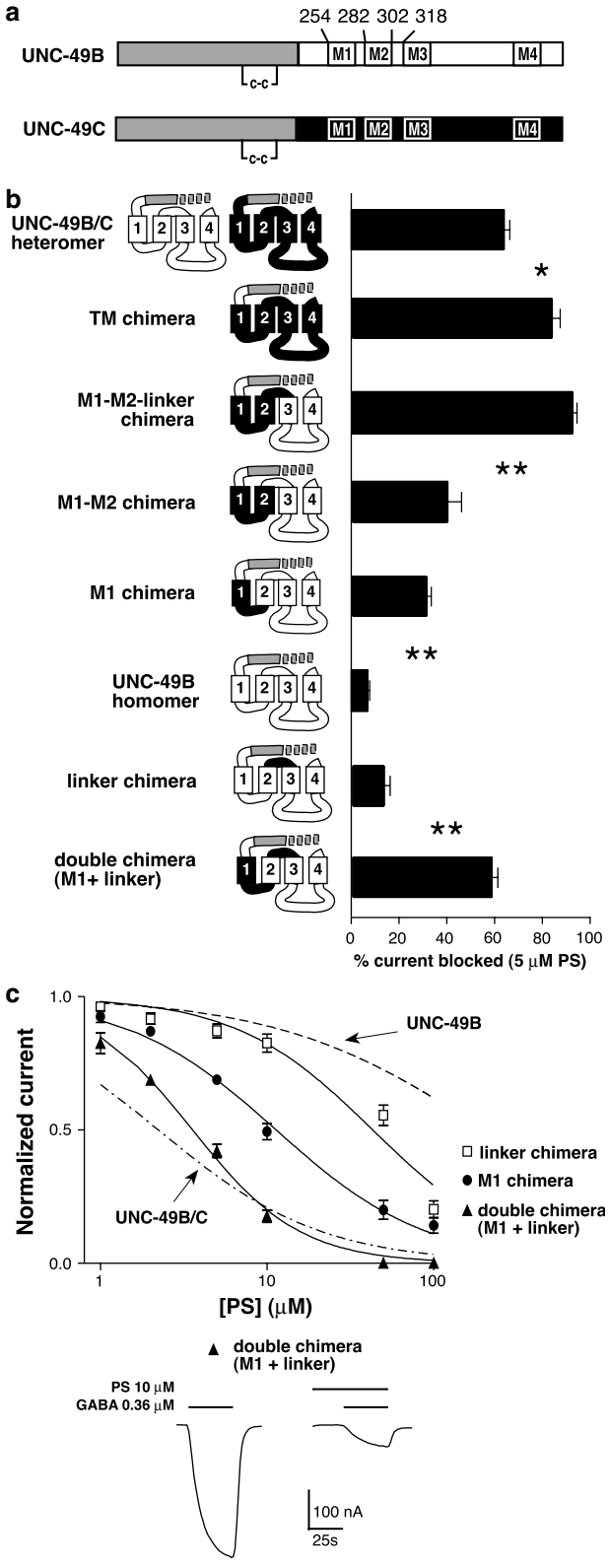

Conserved M1 and M2–M3 linker residues contribute to PS sensitivity

Which residues in these regions are responsible for PS sensitivity? In our second step, we identified amino acids in these regions that were conserved among neurosteroid-sensitive GABA$_A$ receptors and UNC-49C but differed in UNC-49B (Figure 3a, and Methods). Within the M2–M3 linker, most residues are conserved among all GABA receptor subunits. However, mammalian GABA$_A$ receptor subunits and UNC-49C contain one or two positively charged residues at the extracellular end of the pore-forming M2 helix (Figure 3a). By contrast, UNC-49B contains only neutral residues in this region (N304, N305, S306). To test the function of residues in the M2–M3 linker, we mutated asparagine 305 to arginine in the M1 chimera to create the 'M1-R' subunit, and compared it to the double chimera containing both the M1 and linker regions (Figure 3b). The N305R mutation increases the PS sensitivity to the same level as in the double chimera (Figure 3b, Table 1). Therefore, we conclude that a single positively charged residue is sufficient to account for the ability of the UNC-49C M2–M3 linker to confer heightened PS sensitivity.

We tested the conserved residues in the UNC-49C M1 domain in a similar way. Two residues in the M1 domain are conserved among the mammalian GABA receptor subunits and UNC-49C but differ from UNC-49B. Specifically, residues 259 and 261 are glutamine and an aromatic residue, respectively, in the PS-sensitive subunits, but these residues are asparagine and valine in the UNC-49B M1 domain. To test the importance of these conserved residues, we substituted them into an UNC-49B subunit with the linker mutation N305R to create the 'QF-R' subunit (Figure 3c). This receptor is 2.1-fold more sensitive to PS than N305R, but it is still 6.7-fold less sensitive than the double chimera (Figure 3c, Table 1). We conclude that residues 259 and 261 are important but that other residues in M1 also play a role.

Figure 2 M1, and the M2–M3 extracellular linker contain determinants of PS sensitivity. (a) UNC-49B and UNC-49C contain 188 identical N-terminal amino acids (gray), but different C-terminal regions (white for UNC-49B, black for UNC-49C). 'c–c' indicates the conserved cysteine loop, M1–M4 indicate transmembrane domains, and numbers above UNC-49B indicate chimera junctions shown in (b). Note that the M1 chimera contains the M1–M2 linker from UNC-49C. (b) Chimeric subunits comprising UNC-49B (white) and UNC-49C (black) sequences are differentially sensitive to PS inhibition. The UNC-49C M1 and M2–M3 linker domains are necessary for high PS sensitivity ($n \geqslant 3$ oocytes for each molecule). Asterisks are placed between each pair of adjacent columns that differ significantly (*$P<0.01$, **$P<0.001$, one-way ANOVA with Tukey's multiple comparison test; $n \geqslant 3$ for each chimera). (c) PS dose–response curve for the linker, M1, and double chimeras. PS inhibition was measured at the GABA EC$_{50}$ for each subunit ($n=4$ oocytes). Representative traces showing the inhibition of the double chimera (M1 + linker) by 10 μM PS are shown below the PS dose–response curves.

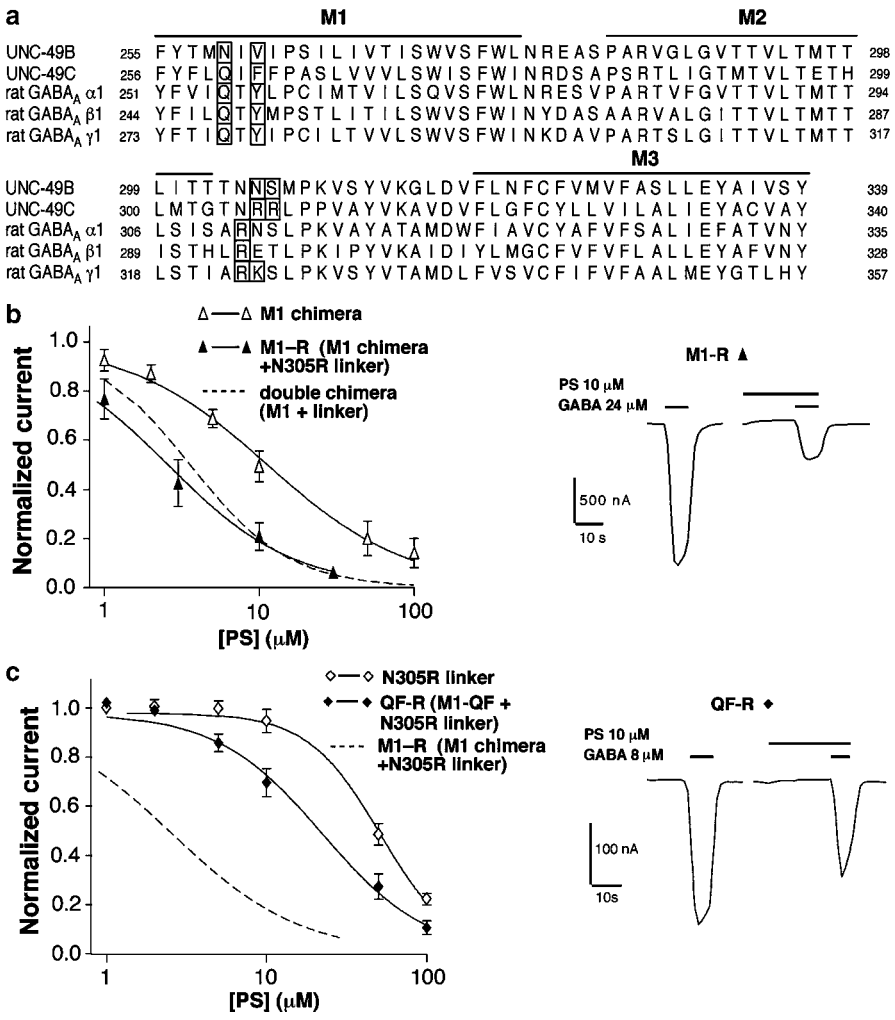

Figure 3 Conserved amino acids in M1 and the M2–M3 linker mediate PS sensitivity. (a) Alignment of UNC-49B, UNC-49C, and the GABA$_A$ receptor α, β, and γ subunits. Bars indicate the positions of transmembrane domains. Boxed residues are conserved in UNC-49C and the vertebrate receptors, but differ in UNC-49B. Alignment is shown with a subset of receptors which were compared to illustrate conserved and divergent residues (see Methods). (b) PS dose–response curves comparing the M1 chimera (open triangles) and M1-R subunit (closed triangles; $n=4$ oocytes for each receptor). (c) PS dose–response curves for the N305R subunit (open diamonds), and the QF-R subunit (closed diamonds; $n=4$ oocytes for each receptor). Dashed line is the M1-R PS dose–response curve, replotted from (b). Representative traces showing the inhibition of the M1-R and QF-R receptors by 10 μM PS are shown next to the PS dose–response curves in (b) and (c), respectively. PS responses were measured at the EC_{50} GABA concentration for each subunit.

Additional M1 residues influence PS sensitivity

In our third step, we identified other nonconserved residues in UNC-49C that were providing full PS sensitivity to this subunit. We subdivided the UNC-49C M1 domain into three segments of roughly equal length, called X, Y, and Z, and tested them for the ability to increase PS sensitivity of the QF-R receptor (Figure 4a). No domain alone was sufficient (top three chimeras, Figure 4b). High PS sensitivity required both the X and Y segments, while Z was dispensible. Interestingly, there is an incompatibility between mixed X and Y segments. Specifically, the X domain from QF-R juxtaposed to the Y domain from UNC-49C eliminates PS sensitivity (Y and YZ chimeras). This observation suggests that residues in the X and Y segments must work together to confer high sensitivity to PS inhibition.

To identify the nonconserved residues within M1 required for maximal PS sensitivity, we determined the specific residues in the X and Y segments that provided maximal PS sensitivity (Figure 5). First, we used the X chimera background to ascertain which Y segment residues caused the 3.7-fold increase in PS sensitivity seen in the XY chimera. Five residues differ between UNC-49B and UNC-49C within this segment and only these residues are shown in Figure 5a. The serine at position 265 was sufficient to confer full PS sensitivity; no other residue in the Y segment increased PS sensitivity.

Important residues in the X segment were tested by substituting UNC-49C residues into the Y chimera. Six residues differ between UNC-49C and UNC-49B within the X segment, including the 'QF' conserved residues 259 and 261 (Figure 5b). We tested these divergent X segment residues by mutating them from UNC-49B to UNC-49C amino acids in the Y chimera background. All mutants were constructed with UNC-49C 'QF' residues at 259 and 261, in order to cut down on the number of possible combinations that we needed to test (from 62 to 14). The remaining four residues (257, 258, 262,

and 264) were substituted in all possible single, double, and triple mutant combinations. The results of this experiment revealed that maximal PS sensitivity required all four of these UNC-49C amino acids. The most important UNC-49C residues were at positions 257 and 262, while the substitutions at position 264 had little effect. Surprisingly, mutating residue 258 in certain combinations confers a biphasic response. At high PS levels (100 μM) GABA-gated currents are inhibited like the relatively insensitive starting construct, the Y chimera. However, moderate levels of PS (10 μM) enhance GABA-

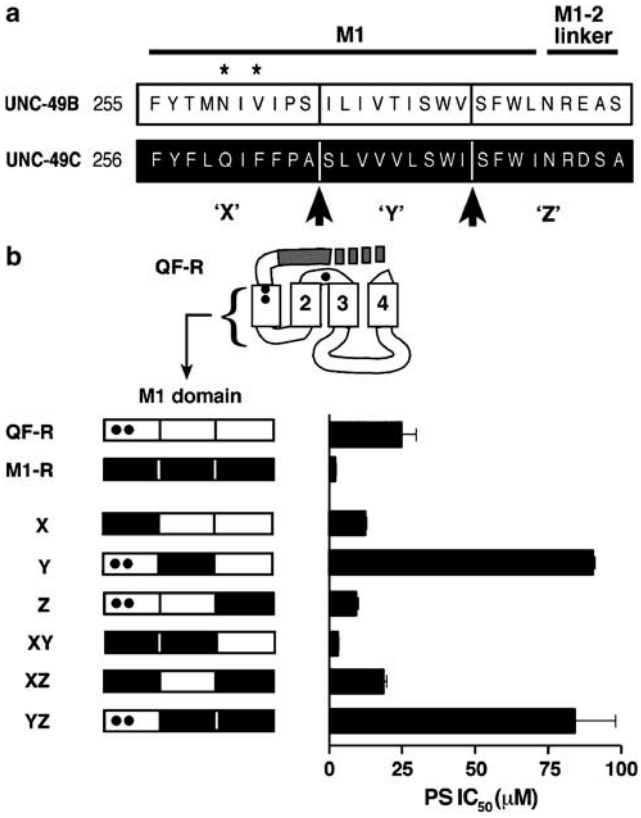

Figure 4 Localization of residues important for PS inhibition within M1. (a) Subdivision of the M1 domain, including the M1–M2 linker, into three segments, designated X, Y, and Z. Asterisks indicate conserved residues at positions 259 and 261, arrows represent boundaries of the X segment (residues 255–264), Y segment (residues 265–273), and Z segment (residues 274–282). (b) PS sensitivity of chimeric receptors in which UNC-49C sequences corresponding to the X, Y, and Z segments have been swapped into the QF-R subunit in different combinations. Bars at the left represent the M1 plus M1–M2 linker region in (a). Closed portions are UNC-49C, open are UNC-49B. Black dots represent UNC-49B to UNC-49C mutations at positions 259, 261, and 305. PS IC_{50} values were determined by generating PS dose–response curves at EC_{50} GABA ($n \geqslant 3$ ooctyes for each molecule; Table 2).

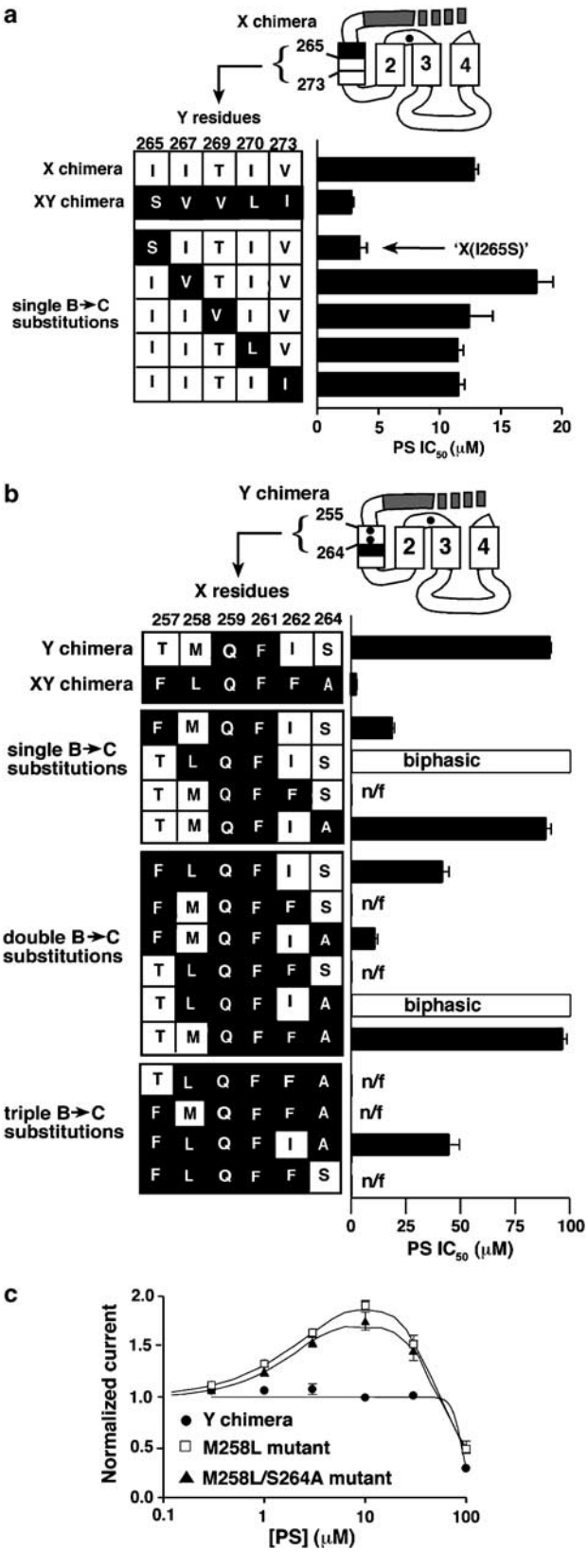

Figure 5 Identification of M1 residues important for PS inhibition. (a) PS sensitivity of Y segment mutants in the X chimera background. Chimeric M1 domain depicted as in Figure 4. Grid indicates the residue present at each position that is divergent between UNC-49B and UNC-49C. Closed boxes and white letters are UNC-49C, open boxes and black letters are UNC-49B. (b) PS sensitivity of X segment mutants in the Y chimera background. Grid indicates residues at divergent positions between UNC-49B and UNC-49C as in (a). 'n/f' indicates nonfunctional. Open bars on bar graph represent biphasic PS dose–responses. Black dots on subunit diagrams in (a) and (b) represent UNC-49B to UNC-49C mutations at positions 259, 261, and 305. (c) Biphasic PS dose–response of mutants containing the M258L mutation, compared to the Y chimera. All PS IC_{50} values and dose-response curves generated at EC_{50} GABA ($n \geqslant 3$ ooctyes for each molecule; Table 3).

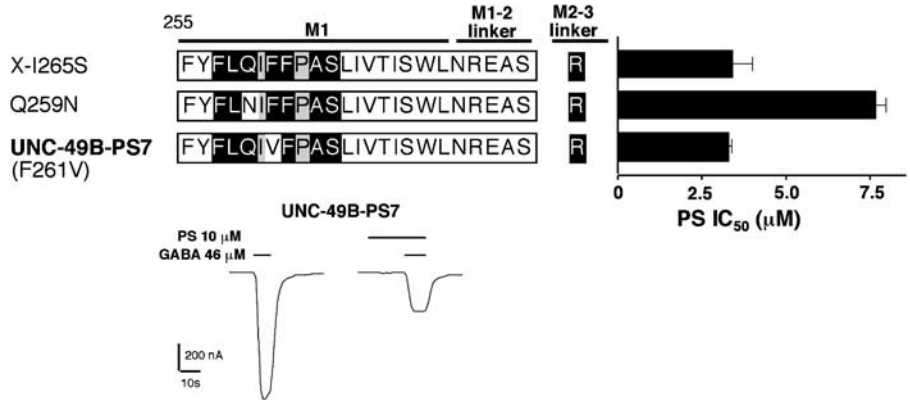

Figure 6 Importance of conserved residues 259 and 261 in M1. The molecule X(I265S) contains a stretch of UNC-49C residues in M1 and an UNC-49B to C substitution in the M2–M3 linker (black letters on white background are UNC-49B residues, white letters on a black background are UNC-49C residues, black letters on a gray background are the same in both subunits). Conserved residues Q259 and F261 were reverted to their UNC-49B amino acids (asparagine and valine, respectively). The Q259N reversion reduced PS sensitivity, but the F261V reversion did not. Therefore, the F261V reversion of X(I265S) contains the minimum number of UNC-49C residues (seven) required to produce high PS sensitivity, and is designated UNC-49B-PS7. PS IC_{50} values were measured at EC_{50} GABA for each subunit ($n=4$ oocytes for each molecule, Table 3). Representative traces showing the inhibition of UNC-49B-PS7 by 10 μM PS are shown in the lower panel.

Table 2 GABA and PS responsiveness of M1 chimeras

Subunit	*PS*		*GABA*	
	IC_{50} (μM)	*Slope coefficient*	*EC_{50} (μM)*	*Slope coefficient*
X	12.8±0.3 ($n=4$)[a]	1.0±0.03 ($n=4$)	2.0±0.4 ($n=3$)	1.7±0.6 ($n=3$)
Y	90.8±0.5 ($n=3$)[a]	10.4±1.3 ($n=3$)	18.4±1.3 ($n=4$)	1.4±0.1 ($n=4$)
Z	9.3±0.6 ($n=4$)[a]	1.05±0.03 ($n=4$)	11.2±3.9 ($n=6$)	1.5±0.1 ($n=6$)
XY	3.7±0.5 ($n=7$)[b]	1.6±0.2 ($n=7$)	84.2±9.0 ($n=3$)	6.0±2.5 ($n=3$)
XZ	14.4±1.7 ($n=8$)[c]	1.1±0.06 ($n=8$)	3.1±0.4 ($n=4$)	2.3±0.3 ($n=4$)
YZ	84.4±13.7 ($n=4$)[c]	3.5±1.6 ($n=4$)	15.4±4.7 ($n=3$)	1.4±0.2 ($n=3$)

In addition to UNC-49C M1 sequences indicated, all molecules contained the N305R mutation in the M2–M3 linker. Error values are s.e.m. PS IC_{50} values were determined at EC_{50} GABA.
[a]Significantly different from XY chimera ($P<0.05$, Students' t-test).
[b]Not significantly different from M1-R ($P>0.05$, Student's t-test).
[c]Significantly different from XY chimera ($P<0.05$, Mann–Whitney U-test).

induced currents, a response not observed in any other subunits. Biphasic curves could be accurately fit using the product of an enhancing and an inhibitory Hill equation (Figure 5c), suggesting that in these mutant combinations, the M258L mutation may unmask an enhancing site that can function together with the inhibitory site.

Finally, to determine the minimum number of residues required for PS sensitivity, we re-examined the conserved 'QF' residues at positions 259 and 261 in the context of the maximally responsive receptor 'X(I265S)' presented in Figure 5a. Reverting residue 259 from glutamine (UNC-49C) to asparagine (UNC-49B) caused a 2.2-fold reduction in PS sensitivity, while reverting residue 261 from phenylalanine (UNC-49C) to valine (UNC-49B) had no effect (Figure 6). We named this phenylalanine to valine revertant UNC-49B-PS7. It contains the minimum number of UNC-49C residues (seven) necessary to confer the maximum 58-fold increase in PS sensitivity to the UNC-49B subunit.

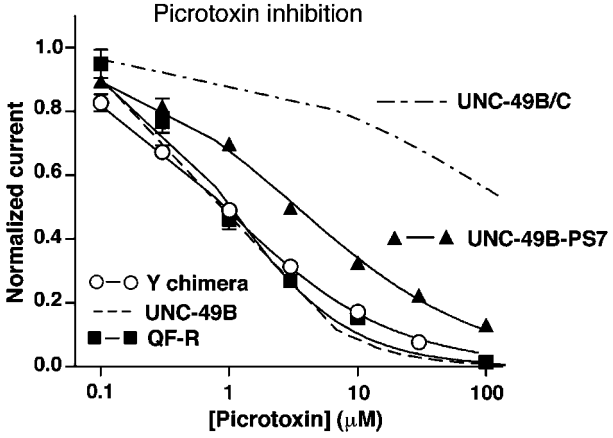

Figure 7 Effects of mutations on picrotoxin sensitivity. Picrotoxin dose–response curves for mutants with varying PS sensitivity. Picrotoxin inhibition is measured at EC_{50} GABA ($n=4$ oocytes for each mutant). Picrotoxin dose–response curves for UNC-49B and UNC-49B/C from Bamber *et al*. (2003).

Other allosteric regulators

Are these residues specific for PS, or do they affect other allosteric regulators of the GABA receptor? We used the allosteric inhibitor picrotoxin to answer this question. Picrotoxin sensitivity did not vary consistently with PS sensitivity among the mutants. For example, the PS sensitivities of the

Table 3 GABA and PS responsiveness of M1 point mutants

Subunit	*PS*		*GABA*	
	IC_{50} (μM)	*Slope coefficient*	EC_{50} (μM)	*Slope coefficient*
X(I265S)	3.43±0.6 ($n=6$)[a]	1.1±0.1 ($n=6$)	49.2±5.8 ($n=3$)	0.8±0.1 ($n=3$)
X(I267V)	17.9±1.4 ($n=3$)[b]	1.1±0.05 ($n=3$)	2.9±0.1 ($n=3$)	1.4±0.7 ($n=3$)
X(T269V)	12.4±1.9 ($n=3$)[c]	1.2±0.1 ($n=3$)	6.5±0.8 ($n=3$)	2.9±0.2 ($n=3$)
X(I270L)	11.5±0.5 ($n=4$)[b]	1.5±0.1 ($n=4$)	0.9±0.2 ($n=3$)	1.4±0.7 ($n=3$)
X(V273I)	11.6±0.5 ($n=3$)[b]	1.0±0.02 ($n=3$)	12.1±0.5 ($n=3$)	3.0±0.3 ($n=3$)
Y(T257F)	18.6±0.9 ($n=4$)[b]	1.3±0.06 ($n=4$)	1.4±0.5 ($n=3$)	0.7±0.07 ($n=3$)
Y(M258L)	100 (biphasic)	ND	249.3±28.5 ($n=5$)	1.2±0.03 ($n=5$)
Y(S264A)	88.7±2.9 ($n=4$)[c]	5.3±1.8 ($n=4$)	24.4±3.3 ($n=3$)	0.8±0.1 ($n=3$)
Y(T257F/M258L)	41.5±3.0 ($n=4$)[c]	2.3±0.2 ($n=4$)	33.4±2.6 ($n=3$)	1.9±0.2 ($n=3$)
Y(T257F/S264A)	10.6±1.9 ($n=4$)[b,d]	0.9±0.08 ($n=4$)	1.2±0.1 ($n=3$)	2.6±0.4 ($n=3$)
Y(M258L/S264A)	100 (biphasic)	ND	256.0±37.6 ($n=4$)	1.22±0.1 ($n=4$)
Y(I262F/S264A)	97.6±1.9 ($n=4$)[c]	11.5±0.3 ($n=3$)	6.3±2.1 ($n=3$)	1.5±0.6 ($n=3$)
Y(T257F/M258L/S264A)	44.4±4.8 ($n=4$)[c]	1.44±0.1 ($n=4$)	12.8±1.3 ($n=3$)	2.3±0.3 ($n=3$)
X(I265S, Q259N)	7.7±0.3 ($n=4$)[e]	0.9±0.0 ($n=4$)	80.4±10.0 ($n=4$)	0.77±0.05 ($n=4$)
UNC-49B-PS7	3.3±0.1 ($n=4$)[f,g]	1.0±0.0 ($n=4$)	46.2±11.1 ($n=4$)	1.06±0.04 ($n=4$)

All molecules contained the N305R mutation in the M2–M3 linker. All molecules, apart from X (I265S, Q259N) and UNC-49B-PS7, contained the two conserved UNC-49C residues at positions 259 and 261. Error values are s.e.m. PS IC_{50} values were determined at EC_{50} GABA.

[a]Not significantly different from XY ($P>0.05$, Student's t-test).
[b]Significantly different from XY ($P<0.05$, Student's t-test).
[c]Significantly different from XY ($P<0.05$, Mann–Whitney U-test).
[d]Significantly different from Y(T257F) ($P<0.05$, Student's t-test).
[e]Significantly different from X(I265S) ($P<0.05$, Mann–Whitney U-test).
[f]Not significantly different from X(I265S) ($P>0.05$, Mann–Whitney U-test).
[g]Not significantly different from M1-R ($P>0.05$, Mann–Whitney U-test).

wild-type UNC-49B, the QF-R subunit, and the Y chimera differ over an eight-fold range (Tables 1 and 2), whereas their picrotoxin sensitivities are identical (Figure 7, and Bamber *et al*., 2003). Conversely, the PS sensitivies of UNC-49B-PS7 and the UNC-49B/C heteromer differ by 1.4-fold (Tables 1 and 3), but their picrotoxin sensitivities differ by 50-fold (Figure 7, Bamber *et al*., 2003). Clearly, other residues in these subunits confer picrotoxin effects. These results provide evidence that the PS-sensitive residues identified here play a specific role in neurosteroid action, and not a general role in allosteric inhibition.

Discussion

We identified domains and residues that mediate GABA receptor inhibition by neurosteroids. We constructed chimeric receptors using sequences from two *C. elegans* subunits, UNC-49B and UNC-49C, which were resistant and sensitive, respectively, to inhibition by PS. We first determined that the M1 domain and the M2–M3 linker of UNC-49C were important for PS inhibition. Mutagenesis experiments revealed six amino acids within the amino-terminal half of M1 that play a dominant role in PS sensitivity. A single residue in the M2–M3 linker was also found to be important. These residues are important for the actions of PS, but not for the actions of another allosteric inhibitor, picrotoxin. Thus, these residues appear to play a specific role in neurosteroid modulation.

The effect of the positively charged residue in the M2–M3 linker on PS responsiveness suggests that PS inhibits the GABA receptor by affecting channel gating. Efficient gating of a related ligand-gated chloride channel, the glycine receptor, requires a positively charged residue in the M2–M3 linker (Rajendra *et al*., 1995). A similar dependence is observed with UNC-49B: wild-type UNC-49B lacks this positively charged residue, and is relatively insensitive to GABA, while introducing this positive charge consistently increased GABA sensitivity. This mutation also increased PS sensitivity, suggesting a mechanistic linkage between gating and PS inhibition. It is possible that the negatively charged sulfate group of PS directly binds the M2–M3 loop to influence gating, in which case, the added positive charge would increase the affinity of PS binding. Alternatively, the effects of this mutation could be indirect. Mutations that add positive charge could influence how receptor residues move relative to one another after GABA binding, such that gating becomes more sensitive to inhibition by PS binding elsewhere.

The M1 domain appears to be the site at which the GABA activation and PS inhibition mechanisms converge. In addition to their importance for PS sensitivity, M1 residues also strongly affect GABA sensitivity. GABA EC_{50} values ranged from 0.9 to 256 μM among receptors containing mutations in the M1 domain (Table 3). These mutations were not in a region that contributes residues to the GABA-binding site, so these variations probably reflect alterations in receptor transitions downstream of GABA binding (Colquhoun, 1998). Several other studies have demonstrated that mutations in M1 affect gating and desensitization in GABA$_A$ receptors and other cysteine-loop receptors (England *et al*., 1999; Dang *et al*., 2000; Bianchi *et al*., 2001). The dual role of M1 in GABA activation and PS inhibition suggests that PS binding to the receptor may alter the position or constrain the motion of the identified M1 residues, with the result that GABA gating becomes impaired. PS could directly bind the M1 domain, or bind elsewhere on the receptor to effect these changes. Our data do not distinguish between a PS binding or transduction role for M1 residues.

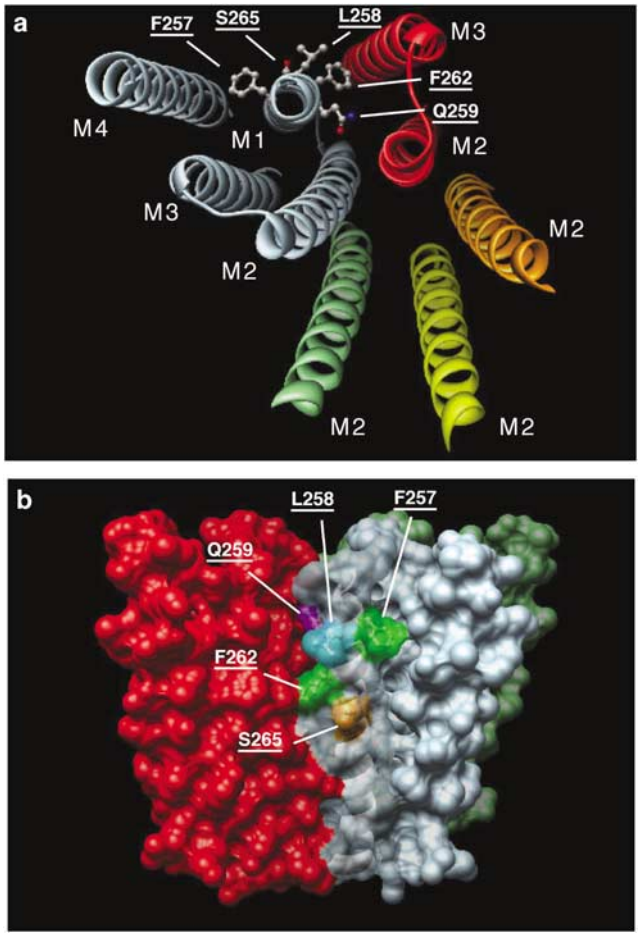

Figure 8 Homology model of UNC-49B, showing residues important for PS inhibition. Model of the UNC-49B homopentamer, with PS-sensitive substitutions in M1, threaded onto the 4 Å structure of the nicotinic acetylcholine receptor (Miyazawa *et al*., 2003). (a) View into the receptor from the outside of the cell. Transmembrane helices are shown as ribbons, residues identified as important for PS inhibition are shown as ball-and-stick representations. Helices in grey belong to a single subunit; two of the four helices of the adjacent subunit shown in red, M2 helices only of the three remaining subunits are shown. (b) View in the plane of the membrane showing surface representation of UNC-49B. Residues important for PS inhibition are indicated and colored (LEU, cyan; SER, orange; PHE, green; GLN, purple). Color scheme corresponds to subunit colors in (a).

The recently published structure of the nicotinic acetylcholine receptor, a homolog of the GABA$_A$ receptor, suggests a potential mechanism for the modulation of gating by PS (Miyazawa *et al*., 2003). We have constructed a homology model of the GABA$_A$ receptor based on the nicotinic receptor (Figure 8). The side chains along one face of M2 line the channel pore; the opposite side of M2 transmembrane domain is apposed to the M1 domain. Opening of the channel is believed to involve rotation of the M2 helices of the five subunits (Miyazawa *et al*., 2003). PS binding to the receptor might reposition M1, altering its interaction with M2 side chains to favor closed states. Our studies showed that M1 residues L258, Q259, F262, and S265 are important for PS responsiveness. In fact, the side chain of residue Q259 is predicted to be oriented toward the M2 helix, and could mediate an interaction between M1 and M2. By contrast, the side chains of L258 and S265 are oriented away from the other transmembrane helices. S265 lies within the cell membrane and is exposed to membrane lipids. Therefore, it might bind the hydrophobic moieties of PS that are stable within the cell membrane. L258 is predicted to lie at the extracellular boundary of the cell membrane. Therefore, this residue could interact with PS atoms nearer to the negatively charged sulfate group, which is presumably forced to remain in contact with the hydrophilic extracellular environment.

Previous studies of GABA$_A$ and glycine receptors had identified important residues in the M1, M2, and M3 domains for allosteric regulation (Ffrench-Constant *et al*., 1993; Belelli *et al*., 1997; Mihic *et al*., 1997; Carlson *et al*., 2000). Mutating these residues in certain GABA receptor subunits also affects neurosteroid modulation (Akk *et al*., 2001; Chang *et al*., 2003; Morris & Amin, 2004), indicating that neurosteroids and other drugs share some mechanisms of allosteric regulation in common. By contrast the residues identified in this study do not seem to mediate the effects of picrotoxin, suggesting that the identified residues are specifically involved in neurosteroid modulation, and not in the actions of unrelated modulators.

We thank Matt Jones for critical reading and assistance with curve fitting. This work was supported by NIH Grants NS43345 and MH64699 (B.A.B.), NS35307 (E.M.J.), the Klingenstein Fund (E.M.J.), and a gift from the Pfizer Corporation (B.A.B.).

References

AKK, G., BRACAMONTES, J. & STEINBACH, J.H. (2001). Pregnenolone sulfate block of GABA(A) receptors: mechanism and involvement of a residue in the M2 region of the alpha subunit. *J. Physiol.,* **532,** 673–684.

BAMBER, B.A., BEG, A.A., TWYMAN, R.E. & JORGENSEN, E.M. (1999). The *Caenorhabditis elegans unc-49* locus encodes multiple subunits of a heteromultimeric GABA receptor. *J. Neurosci.,* **19,** 5348–5359.

BAMBER, B.A., RICHMOND, J.E., OTTO, J.F. & JORGENSEN, E.M. (2005). Composition of the GABA receptor at the *Caenorhabditis elegans* neuromuscular junction. *Br. J. Pharmacol.,* **144,** 502–509.

BAMBER, B.A., TWYMAN, R.E. & JORGENSEN, E.M. (2003). Pharmacological characterization of the homomeric and heteromeric UNC-49 GABA receptors in *C. elegans*. *Br. J. Pharmacol.,* **138,** 883–893.

BELELLI, D. & LAMBERT, J.J. (2005). Neurosteroids: endogenous regulators of the GABA(A) receptor. *Nat. Rev. Neurosci.,* **6,** 565–575.

BELELLI, D., LAMBERT, J.J., PETERS, J.A., WAFFORD, K. & WHITING, P.J. (1997). The interaction of the general anesthetic etomidate with the gamma-aminobutyric acid type A receptor is influenced by a single amino acid. *Proc. Natl. Acad. Sci. U.S.A.,* **94,** 11031–11036.

BIANCHI, M.T., HAAS, K.F. & MACDONALD, R.L. (2001). Structural determinants of fast desensitization and desensitization–deactivation coupling in GABA$_A$ receptors. *J. Neurosci.,* **21,** 1127–1136.

CARLSON, B.X., ENGBLOM, A.C., KRISTIANSEN, U., SCHOUSBOE, A. & OLSEN, R.W. (2000). A single glycine residue at the entrance to the first membrane-spanning domain of the gamma-aminobutyric acid type A receptor beta(2) subunit affects allosteric sensitivity to GABA and anesthetics. *Mol. Pharmacol.,* **57,** 474–484.

CHANG, C.S., OLCESE, R. & OLSEN, R.W. (2003). A single M1 residue in the beta2 subunit alters channel gating of GABA$_A$ receptor in anesthetic modulation and direct activation. *J. Biol. Chem.,* **278,** 42821–42828.

COLQUHOUN, D. (1998). Binding, gating, affinity and efficacy: the interpretation of structure-activity relationships for agonists and of the effects of mutating receptors. *Br. J. Pharmacol.,* **125,** 924–947.

DANG, H., ENGLAND, P.M., FARIVAR, S.S., DOUGHERTY, D.A. & LESTER, H.A. (2000). Probing the role of a conserved M1 proline residue in 5-hydroxytryptamine(3) receptor gating. *Mol. Pharmacol.,* **57,** 1114–1122.

ENGLAND, P.M., ZHANG, Y., DOUGHERTY, D.A. & LESTER, H.A. (1999). Backbone mutations in transmembrane domains of a ligand-gated ion channel: implications for the mechanism of gating. *Cell,* **96,** 89–98.

FFRENCH-CONSTANT, R.H., ROCHELEAU, T.A., STEICHEN, J.C. & CHALMERS, A.E. (1993). A point mutation in a *Drosophila* GABA receptor confers insecticide resistance. *Nature,* **363,** 449–451.

GASIOR, M., CARTER, R.B. & WITKIN, J.M. (1999). Neuroactive steroids: potential therapeutic use in neurological and psychiatric disorders. *Trends Pharmacol. Sci.,* **20,** 107–112.

JONES, M.V., JONAS, P., SAHARA, Y. & WESTBROOK, G.L. (2001). Microscopic kinetics and energetics distinguish GABA(A) receptor agonists from antagonists. *Biophys. J.,* **81,** 2660–2670.

KERRIGAN, J.F., SHIELDS, W.D., NELSON, T.Y., BLUESTONE, D.L., DODSON, W.E., BOURGEOIS, B.F., PELLOCK, J.M., MORTON, L.D. & MONAGHAN, E.P. (2000). Ganaxolone for treating intractable infantile spasms: a multicenter, open-label, add-on trial. *Epilepsy Res.,* **42,** 133–139.

LAXER, K., BLUM, D., ABOU-KHALIL, B.W., MORRELL, M.J., LEE, D.A., DATA, J.L. & MONAGHAN, E.P. (2000). Assessment of ganaxolone's anticonvulsant activity using a randomized, double-blind, presurgical trial design. Ganaxolone Presurgical Study Group. *Epilepsia,* **41,** 1187–1194.

LESTER, H.A., DIBAS, M.I., DAHAN, D.S., LEITE, J.F. & DOUGHERTY, D.A. (2004). Cys-loop receptors: new twists and turns. *Trends Neurosci.,* **27,** 329–336.

MACDONALD, R.L. & OLSEN, R.W. (1994). GABA$_A$ receptor channels. *Ann. Rev. Neurosci.,* **17,** 569–602.

MAJEWSKA, M.D. (1992). Neurosteroids: endogenous bimodal modulators of the GABA$_A$ receptor. Mechanism of action and physiological significance. *Prog. Neuorobiol,* **38,** 379–395.

MELLON, S.H. & GRIFFIN, L.D. (2002). Neurosteroids: biochemistry and clinical significance. *Trends Endocrinol. Metab.,* **13,** 35–43.

MIHIC, S.J., YE, Q., WICK, M.J., KOLTCHINE, V.V., KRASOWSKI, M.D., FINN, S.E., MASCIA, M.P., VALENZUELA, C.F., HANSON, K.K., GREENBLATT, E.P., HARRIS, R.A. & HARRISON, N.L. (1997). Sites of alcohol and volatile anaesthetic action on GABA$_A$ and glycine receptors. *Nature,* **389,** 385–389.

MIYAZAWA, A., FUJIYOSHI, Y. & UNWIN, N. (2003). Structure and gating mechanism of the acetylcholine receptor pore. *Nature,* **423,** 949–955.

MORRIS, K.D. & AMIN, J. (2004). Insight into the mechanism of action of neuroactive steroids. *Mol. Pharmacol.,* **66,** 56–69.

MORROW, A.L., KHISTI, R., TOKUNAGA, S., MCDANIEL, J.R. & MATTHEWS, D.B. (2004). GABAergic neuroactive steroids modulate selective ethanol actions: mechanisms and significance. In *Neurosteroid Effects in the Central Nervous System*. ed. Smith, S.S., pp. 219–245. Boca Raton, FL: CRC Press.

NILSSON, K.R., ZORUMSKI, C.F. & COVEY, D.F. (1998). Neurosteroid analogues. 6. The synthesis and GABA$_A$ receptor pharmacology of enantiomers of dehydroepiandrosterone sulfate, pregnenolone sulfate, and (3α, 5β)-3-hydroxypregnan-20-one sulfate. *J. Med. Chem.,* **41,** 2604–2613.

OLSEN, R.W. & TOBIN, A.J. (1990). Molecular biology of GABA$_A$ receptors. *FASEB J.,* **4,** 1469–1480.

PARK-CHUNG, M., MALAYEV, A., PURDY, R.H., GIBBS, T.T. & FARB, D.H. (1999). Sulfated and unsulfated steroids modulate gamma-aminobutyric acidA receptor function through distinct sites. *Brain Res.,* **830,** 72–87.

PAUL, S.M. & PURDY, R.H. (1992). Neuroactive steroids. *FASEB J.,* **6,** 2311–2322.

RAJENDRA, S., LYNCH, J.W., PIERCE, K.D., FRENCH, C.R., BARRY, P.H. & SCHOFIELD, P.R. (1995). Mutation of an arginine residue in the human glycine receptor transforms beta-alanine and taurine from agonists into competitive antagonists. *Neuron,* **14,** 169–175.

RUPPRECHT, R. (2003). Neuroactive steroids: mechanisms of action and neuropsychopharmacological properties. *Psychoneuroendocrinology,* **28,** 139–168.

SALI, A. & BLUNDELL, T.L. (1993). Comparative protein modelling by satisfaction of spatial restraints. *J. Mol. Biol.,* **234,** 779–815.

SHEN, W., MENNERICK, S., ZORUMSKI, E.C., COVEY, D.F. & ZORUMSKI, C.F. (1999). Pregnenolone sulfate and dehydroepiandrosterone sulfate inhibit GABA-gated chloride currents in *Xenopus* oocytes expressing picrotoxin-insensitive GABA$_A$ receptors. *Neuropharmacology,* **38,** 267–271.

THOMPSON, J.D., HIGGINS, D.G. & GIBSON, T.J. (1994). CLUSTAL W: improving the sensitivity of progressive multiple sequence alignment through sequence weighting, position-specific gap penalties and weight matrix choice. *Nucl. Acids Res.,* **22,** 4673–4680.

VALLEE, M., MAYO, W., DARNAUDERY, M., CORPECHOT, C., YOUNG, J., KOEHL, M., LE MOAL, M., BAULIEU, E.E., ROBEL, P. & SIMON, H. (1997). Neurosteroids: deficient cognitive performance in aged rats depends on low pregnenolone sulfate levels in the hippocampus. *Proc. Natl. Acad. Sci. U.S.A.,* **94,** 14865–14870.

WU, F.S., GIBBS, T.T. & FARB, D.H. (1991). Pregnenolone sulfate: a positive allosteric modulator at the *N*-methyl-D-aspartate receptor. *Mol. Pharmacol.,* **40,** 333–336.

ZAMAN, S.H., SHINGAI, R., HARVEY, R.J., DARLISON, M.G. & BARNARD, E.A. (1992). Effects of subunit types of the recombinant GABA$_A$ receptor on the response to a neurosteroid. *Eur. J. Pharmacol.,* **225,** 321–330.

(Received November 8, 2005
Revised January 20, 2006
Accepted January 25, 2006
Published online 20 March 2006)